

Determining the K_{l3} form factors directly at zero momentum transfer

P.A. Boyle, C. Kelly, C.M. Maynard, J.M. Zanotti*

School of Physics and Astronomy, University of Edinburgh, Edinburgh EH9 3JZ, UK

J.M. Flynn, H. Pedroso de Lima, C.T. Sachrajda

School of Physics and Astronomy, University of Southampton, Southampton SO17 1BJ, UK

A. Jüttner

Institut für Kernphysik, Johannes-Gutenberg Universität Mainz, D-55099 Mainz, Germany

RBC and UKQCD Collaborations

We compute the K_{l3} form factors using partially twisted boundary conditions. The twists are chosen so that the K_{l3} form factors are calculated directly at zero momentum transfer ($q^2 = 0$), removing the need for a q^2 interpolation. The simulations are performed on an ensemble of the RBC/UKQCD collaboration's gauge configurations with Domain Wall Fermions and the Iwaski gauge action with an inverse lattice spacing of 1.73(3) GeV. For the value of the K_{l3} form factor, $f_+^{K\pi}(q^2)$, determined directly at $q^2 = 0$, we find a value of $f_+^{K\pi}(0) = 0.9757(38)$ at this particular quark mass, which agrees well with our earlier result (0.9774(35)) obtained using the standard, indirect method.

The XXVII International Symposium on Lattice Field Theory - LAT2009

July 26-31 2009

Peking University, Beijing, China

*Speaker.

1. Introduction

Over the last few years as part of our Domain Wall Fermion (DWF) physics programme we have been looking at the $K \rightarrow \pi \ell \nu_\ell$ ($K_{\ell 3}$) form factor at zero momentum transfer. Since the experimental rate for $K_{\ell 3}$ decays is proportional to $|V_{us}|^2 |f_+^{K\pi}(0)|^2$, a lattice calculation of the form factor, $f_+^{K\pi}(q^2)$ at $q^2 = 0$, provides an excellent avenue for the determination of the Cabibbo-Kobayashi-Maskawa (CKM) [1] quark mixing matrix element, $|V_{us}|$.

The uncertainty in the unitarity relation of the CKM matrix $|V_{ud}|^2 + |V_{us}|^2 = 1$ (we ignore $|V_{ub}|$ since it is very small), is dominated by the precision of $|V_{us}|$. In Fig. 1 we show the latest determinations of $|V_{ud}|$ [2] and $|V_{us}|$ [3]. For comparison, we also show the unitarity relation. Since it is important to establish unitarity with the best precision possible, it is essential that we decrease the error in $|V_{us}|$.

The value of $f_+^{K\pi}(0)$ used in determining $|V_{us}|$ in figure 1 was determined using standard methods [4, 5] involving periodic spatial boundary conditions for the finite volume quark fields in the recent paper [3]. There, the $K_{\ell 3}$ form factor is calculated at $q_{max}^2 = (m_K - m_\pi)^2$ and several negative values of q^2 for a variety of quark masses. This allows for an interpolation of the results to $q^2 = 0$. The form factor is then chirally extrapolated to the physical pion and kaon masses. The final result for $f_+^{K\pi}(0)$ quoted is then [3] $f_+^{K\pi}(0) = 0.9644(33)(34)(14)$ where the first error is statistical, and the second and third are estimates of the systematic errors due to the choice of q^2 and quark mass parametrisation and lattice artefacts, respectively. Using the result for $|f_+^{K\pi} V_{us}|$ by [6] this gives us a value of $|V_{us}| = 0.2249(14)$.

More recently, we have developed a method that uses partially twisted boundary conditions to calculate the $K_{\ell 3}$ form factor directly at $q^2 = 0$ [7], thereby removing the systematic error due to the choice of parametrisation for the interpolation in q^2 . The method was developed and tested in [7] and now applied in a simulation with parameters much closer to the physical point.

In this paper we discuss our progress in improving the precision of our result for $f_+^{K\pi}(0)$ from [3] using partially twisted boundary conditions. Finally, the systematic due to the chiral extrapolation in the above result includes a correction for the fact that the simulated strange quark has a mass which is a little heavier than the physical one - here we confirm this estimate by new simulation results which allow us to interpolate directly in the strange quark mass.

2. Simulation Parameters

The computations are performed using an ensemble with light quark mass $am_u = am_d = 0.005$ and strange quark mass $am_s = 0.04$ from a set of $N_f = 2 + 1$ flavour DWF configurations with

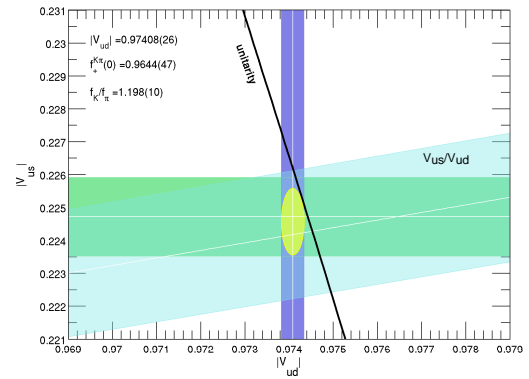


Figure 1: Bands showing the current limits on $|V_{ud}|$ [2], and $|V_{us}|$ [3].

$(L/a)^3 \times T/a \times L_s = 24^3 \times 64 \times 16$ which were jointly generated by the UKQCD/RBC collaborations [8] using the QCDOC computer. The simulated dynamical strange quark mass, $am_s = 0.04$, is close to its physical value [8], while for the valence strange quark mass, we choose two values, $am_s = 0.04$ and $am_s = 0.03$.

The gauge configurations were generated with the Iwasaki gauge action with an inverse lattice spacing of $a^{-1} = 1.729(28)\text{GeV}$. The resulting pion and kaon masses are $m_\pi \approx 330\text{MeV}$ and $m_K \approx 575\text{MeV}$, respectively.

In this work we use single time-slice stochastic sources [9], for which the elements of the source are randomly drawn from a distribution $\mathcal{D} = \mathbb{Z}(2) \otimes \mathbb{Z}(2)$ which contains random $\mathbb{Z}(2)$ numbers in both its real and imaginary parts. With sources of this form we find that the computational cost of calculating quark propagators is reduced by a factor of 12. For more details on the simulations, see [10].

3. The Form Factors

Here we briefly outline the main features of our method and we refer the reader to our earlier papers for more details [3, 7, 10].

The matrix element of the vector current between initial and final state pseudoscalar mesons P_i and P_f , is in general decomposed into two invariant form factors:

$$\langle P_f(p_f) | V_\mu | P_i(p_i) \rangle = f_{P_i P_f}^+(q^2) (p_i + p_f)_\mu + f_{P_i P_f}^-(q^2) (p_i - p_f)_\mu, \quad (3.1)$$

where $q^2 = -Q^2 = (p_i - p_f)^2$. For $K \rightarrow \pi$, $V_\mu = \bar{s}\gamma_\mu u$, $P_i = K$ and $P_f = \pi$. The form factors $f_{P_i P_f}^+(q^2)$ and $f_{P_i P_f}^-(q^2)$ contain the non-perturbative QCD effects and hence are ideally suited for a determination in lattice QCD.

In a finite volume with spatial extent L and periodic boundary conditions for the quark fields, momenta are discretised in units of $2\pi/L$, and the momentum transfer is given by

$$q^2 = (E_K(\vec{p}_i) - E_\pi(\vec{p}_f))^2 - (\vec{p}_i - \vec{p}_f)^2. \quad (3.2)$$

For $\vec{p}_i = 0$ and $2\pi/L$ with $\vec{p}_f = 0$, we have $q^2 \approx 0.06 \text{ GeV}^2$ and -0.05 GeV^2 , respectively, presenting the need for an interpolation in order to extract the result of the form factor, $f_+^{K\pi}$, at $q^2 = 0$.

In order to reach zero momentum transfer ($q^2 = 0$), we employ partially twisted boundary conditions [11, 12], combining gauge field configurations generated with sea quarks obeying periodic boundary conditions with valence quarks with twisted boundary conditions [11–17]. The valence quarks, q , satisfy

$$q(x_k + L) = e^{i\vec{\theta}_k} q(x_k), \quad (k = 1, 3), \quad (3.3)$$

where $\vec{\theta}$ is the twisting angle. Our method is described in detail in [7, 10] and proceeds by setting $\vec{\theta} = 0$ for the spectator quark. We are then able to vary the twisting angles, $\vec{\theta}_i$ and $\vec{\theta}_f$, of the quarks before and after the insertion of the current, respectively. The momentum transfer between the initial and final state mesons is now

$$q^2 = (E_i(\vec{p}_i, \vec{\theta}_i) - E_f(\vec{p}_f, \vec{\theta}_f))^2 - ((\vec{p}_i + \vec{\theta}_i/L) - (\vec{p}_f + \vec{\theta}_f/L))^2, \quad (3.4)$$

where $E(\vec{p}, \vec{\theta}) = \sqrt{m^2 + (\vec{p} + \vec{\theta}/L)^2}$. Hence it is possible to choose $\vec{\theta}_i$ and $\vec{\theta}_f$ such that $q^2 = 0$, which from now on we refer to as $\vec{\theta}_K$ and $\vec{\theta}_\pi$ for when we twist a quark in the Kaon and Pion, respectively.

In order to extract the matrix elements (3.1) from a lattice simulation, we consider the following ratios of three- and two-point correlation functions

$$\begin{aligned} R_{1, P_i P_f}(\vec{p}_i, \vec{p}_f) &= 4\sqrt{E_i E_f} \sqrt{\frac{C_{P_i P_f}(t, \vec{p}_i, \vec{p}_f) C_{P_f P_i}(t, \vec{p}_f, \vec{p}_i)}{C_{P_i}(t_{\text{sink}}, \vec{p}_i) C_{P_f}(t_{\text{sink}}, \vec{p}_f)}}, \\ R_{3, P_i P_f}(\vec{p}_i, \vec{p}_f) &= 4\sqrt{E_i E_f} \frac{C_{P_i P_f}(t, \vec{p}_i, \vec{p}_f)}{C_{P_f}(t_{\text{sink}}, \vec{p}_f)} \sqrt{\frac{C_{P_i}(t_{\text{sink}}-t, \vec{p}_i) C_{P_f}(t, \vec{p}_f) C_{P_f}(t_{\text{sink}}, \vec{p}_f)}{C_{P_f}(t_{\text{sink}}-t, \vec{p}_f) C_{P_i}(t, \vec{p}_i) C_{P_i}(t_{\text{sink}}, \vec{p}_i)}}. \end{aligned} \quad (3.5)$$

We deviate slightly from the method outlined in [7] for extracting $f_0^{K\pi}(0)$ from the ratios. Previously we considered only the time-component of the vector current and solved for $f_0^{K\pi}(0) = f_+^{K\pi}(0)$ via the linear combination

$$f_0^{K\pi}(0) = \frac{R_{\alpha, K\pi}(\vec{p}_K, \vec{0})(m_K - E_\pi) - R_{\alpha, K\pi}(\vec{0}, \vec{p}_\pi)(E_K - m_\pi)}{(E_K + m_\pi)(m_K - E_\pi) - (m_K + E_\pi)(E_K - m_\pi)} \quad (\alpha = 1, 2, 3). \quad (3.6)$$

This, however, is just one of many expressions that can be obtained when we solve the system of simultaneous equations that are obtained when we consider all components of the vector current, V_μ , rather than just V_4 that was considered in [7]

$$\begin{aligned} R_{\alpha, K\pi}(\vec{\theta}_K, \vec{0}, V_4) &= f_+^{K\pi}(0)(E_K + m_\pi) + f_-^{K\pi}(0)(E_K - m_\pi) \\ R_{\alpha, K\pi}(\vec{0}, \vec{\theta}_\pi, V_4) &= f_+^{K\pi}(0)(m_K + E_\pi) + f_-^{K\pi}(0)(m_K - E_\pi) \\ R_{\alpha, K\pi}(\vec{\theta}_K, \vec{0}, V_i) &= f_+^{K\pi}(0)\theta_{K,i} + f_-^{K\pi}(0)\theta_{K,i} \\ R_{\alpha, K\pi}(\vec{0}, \vec{\theta}_\pi, V_i) &= f_+^{K\pi}(0)\theta_{\pi,i} - f_-^{K\pi}(0)\theta_{\pi,i}, \end{aligned} \quad (3.7)$$

where $i = 1, 2, 3$ in the last two equations. We can now proceed to solve this overdetermined system of equations via χ^2 minimisation.

4. K_{I3} form factor results

As explained in Sec. 3, we calculate the $K \rightarrow \pi$ form factor directly at $q^2 = 0$ by setting the Kaon and Pion in turn to be at rest, while twisting the other one such that $q^2 = 0$. We refer to these twist angles as θ_π and θ_K , respectively. We then get the following equations:

$$\begin{aligned} \langle K(p_K) | V_\mu | \pi(0) \rangle &= f_+^{K\pi}(0) p_{K,\mu} - f_-^{K\pi}(0) p_{K,\mu} \\ \langle K(0) | V_\mu | \pi(p_\pi) \rangle &= f_+^{K\pi}(0) p_{\pi,\mu} + f_-^{K\pi}(0) p_{\pi,\mu} \end{aligned} \quad (4.1)$$

By considering all the μ components simultaneously, we perform a χ^2 minimisation on the overdetermined system of equations to find the values of $f_+^{K\pi}(0)$ and $f_-^{K\pi}(0)$ that best fit the equations.

To obtain the matrix elements (4.1), we consider different combinations of R_1 and R_3 (3.5). We find that all combinations lead to consistent results, with the best combination being that we use R_3 for all matrix elements except for the case where the pion is twisted and we are considering

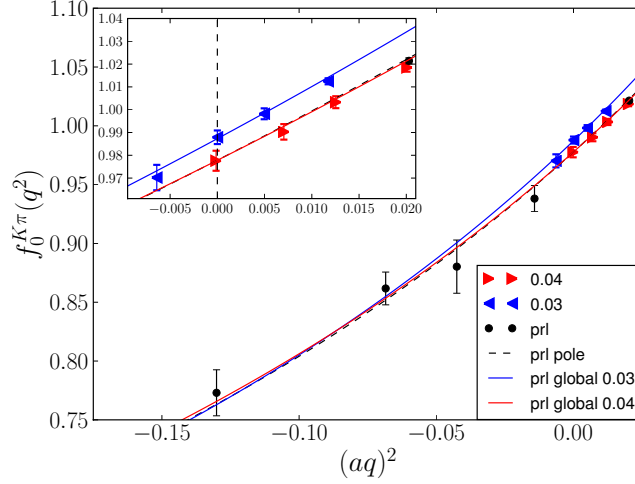


Figure 2: K_{l3} form factor, $f_0^{K\pi}(q^2)$, evaluated at $q^2 = 0$ directly using twisted boundary conditions. Results are compared with data at $q^2 \neq 0$ and fits from [3]

the 4th component of the vector current. Using this set up, we obtain our preliminary results for $f_{K\pi}^+(0)$ and $f_{K\pi}^-(0)$ (for a pion mass of $m_\pi = 330\text{MeV}$)

$$f_{K\pi}^+(0) = 0.9757(38), \quad f_{K\pi}^-(0) = -0.0997(93). \quad (4.2)$$

Our result for $f_{K\pi}^+(0) = f_{K\pi}^0(0)$ is indicated in Fig. 2 by the red right-pointing triangles. We also include additional data points for $f_{K\pi}^+(q^2)$ in the range $0 \lesssim q^2 \leq q_{\text{max}}^2$ obtained using the partially twisted boundary condition technique. These results are compared with the pole dominance fit to the Fourier momentum results (black circles) obtained in [3], as indicated by the dashed black line. As can be seen, this pole dominance fit goes through all of the new partially twisted boundary condition points. In our previous result, $f_{K\pi}^+(0) = 0.9644(33)(34)(14)$, these were combined, taking a systematic error of (34) for the model dependence. This contribution to the error has been eliminated in our new calculation.

4.1 Correcting the strange quark mass

Another source of systematic error in our result in [3] is due to the slight difference between our simulated strange quark mass ($am_s + am_{\text{res}} \simeq 0.043$) and the physical strange quark ($am_s + am_{\text{res}} \simeq 0.037$) [8]. In [3], this was corrected by simultaneously fitting the q^2 and quark mass dependences with the global ansatz

$$f_0^{K\pi}(q^2) = \frac{1 + f_2 + (m_K^2 - m_\pi^2)^2 (A_0 + A_1(m_K^2 + m_\pi^2))}{1 - q^2 / (M_0 + M_1(m_K^2 + m_\pi^2))}, \quad (4.3)$$

to all available data points with four different light quark masses, then inserting in the physical pion and kaon masses to obtain the final result. Using the fit parameters which were determined in [3] and plugging in the unitary and partially quenched kaon mass which we simulated for here, the ansatz in eqn. (4.3) predicts the red and blue curve in figure 2, respectively. Both curves nicely

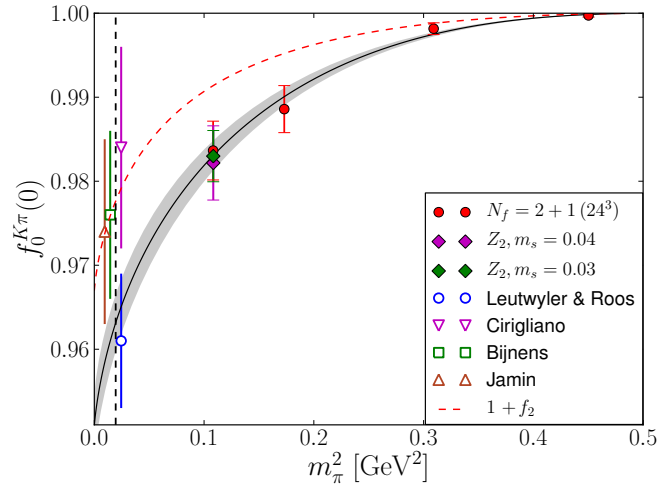


Figure 3: Red points are from [3], while the Z_2 points are from the current analysis. The black curve is from the fit in [3] with Eq. (4.3). All points are shifted to the physical strange quark mass.

fit the red and blue data points. Even though our results for $am_s = 0.03$ were based on partially quenched data, this observation increases our confidence in the semi-phenomenological fit ansatz of [3]. We will need to rely on such ansatz until a NNLO expression for $f_+^{K\pi}(q^2)$ is presented in a closed form as a function of low energy constants and the quark or meson masses.

These two points for $f_+^{K\pi}(0)$ from the $am_l = 0.005$ ensemble with two different strange quark masses are compared in Fig. 3 with the chiral extrapolation from [3]. After shifting all results to the physical strange quark mass, we see again the excellent agreement of the new partially twisted boundary condition results and the earlier results from [3] using more standard techniques.

4.2 Conclusions

We conclude that using partially twisted bc's for the $K_{\ell 3}$ form factor, is an improvement on the conventional method as it removes a source of systematic error, while keeping comparable statistical errors. From calculations with two different valence strange quark masses, we have also shown that effect of simulating with a strange quark mass that differs slightly from its physical value can be easily accounted for by fitting the simulated points with the ansatz (4.3) and inserting the physical pion and kaon masses to obtain the final result.

Simulations at a second lattice spacing and three light masses are currently underway. We also plan to combine our results with the latest expressions from chiral perturbation theory [18].

Acknowledgements

We thank our colleagues in RBC and UKQCD within whose programme this calculation was performed. We thank the QCDOC design team for developing the QCDOC machine and its software. This development and the computers used in this calculation were funded by the U.S.DOE grant DE-FG02-92ER40699, PPARC JIF grant PPA/J/S/1998/0075620 and by RIKEN.

We thank the University of Edinburgh, PPARC, RIKEN, BNL and the U.S. DOE for providing the QCDOC facilities used in this calculation. We are very grateful to the Engineering and Physical Sciences Research Council (EPSRC) for a substantial allocation of time on HECToR under the Early User initiative. We thank Arthur Trew, Stephen Booth and other EPCC HECToR staff for assistance and EPCC for computer time and assistance on BlueGene/L.

JMF, AJ, HPdL and CTS acknowledge support from STFC Grant PP/D000211/1 and from EU contract MRTN-CT-2006-035482 (Flavianet). PAB, CK, CMM acknowledge support from STFC grant PP/D000238/1. JMZ acknowledges support from STFC Grant ST/F009658/1.

References

- [1] N. Cabibbo, Phys. Rev. Lett. **10** (1963) 531; M. Kobayashi and T. Maskawa, Prog. Theor. Phys. **49** (1973) 652.
- [2] W. M. Yao *et al.* [Particle Data Group], J. Phys. G **33** (2006) 1.
- [3] P. A. Boyle *et al.* [RBC/UKQCD], Phys. Rev. Lett. **100** (2008) 141601 [arXiv:0710.5136 [hep-lat]].
- [4] D. Becirevic *et al.*, Nucl. Phys. B **705** (2005) 339 [arXiv:hep-ph/0403217].
- [5] C. Dawson, T. Izubuchi, T. Kaneko, S. Sasaki and A. Soni, Phys. Rev. D **74** (2006) 114502 [arXiv:hep-ph/0607162].
- [6] M. Antonelli *et al.* [FlaviaNet Working Group on Kaon Decays], arXiv:0801.1817 [hep-ph].
- [7] P. A. Boyle *et al.* [RBC/UKQCD], JHEP **0705** (2007) 016 [arXiv:hep-lat/0703005].
- [8] C. Allton *et al.* [RBC/UKQCD], arXiv:0804.0473 [hep-lat].
- [9] P. A. Boyle, A. Juttner, C. Kelly and R. D. Kenway, JHEP **0808** (2008) 086 [arXiv:0804.1501 [hep-lat]].
- [10] P. A. Boyle *et al.* [RBC/UKQCD], JHEP **0807** (2008) 112 [arXiv:0804.3971 [hep-lat]].
- [11] C. T. Sachrajda and G. Villadoro, Phys. Lett. B **609** (2005) 73 [arXiv:hep-lat/0411033].
- [12] P. F. Bedaque and J. W. Chen, Phys. Lett. B **616** (2005) 208 [arXiv:hep-lat/0412023].
- [13] P. F. Bedaque, Phys. Lett. B **593** (2004) 82 [arXiv:nucl-th/0402051].
- [14] G. M. de Divitiis, R. Petronzio and N. Tantalo, Phys. Lett. B **595** (2004) 408 [arXiv:hep-lat/0405002].
- [15] B. C. Tiburzi, Phys. Lett. B **617** (2005) 40 [arXiv:hep-lat/0504002].
- [16] J. M. Flynn, A. Juttner and C. T. Sachrajda [UKQCD], Phys. Lett. B **632** (2006) 313 [arXiv:hep-lat/0506016].
- [17] D. Guadagnoli, F. Mescia and S. Simula, Phys. Rev. D **73** (2006) 114504 [arXiv:hep-lat/0512020].
- [18] J. M. Flynn and C. T. Sachrajda, arXiv:0809.1229 [hep-ph].